

Article

Transformative Spatio-Temporal Insights into Indian Summer Days for Advancing Climate Resilience and Regional Adaptation in India

Deepak Kumar Prajapat ¹, Mahender Choudhary ², Ram Avtar ^{3,4,*}, Saurabh Singh ^{1,3}, Saleh Alsulamy ⁵ and Ali Kharrazi ^{6,7}

- ¹ Department of Civil Engineering, Poornima University, Jaipur 303905, India; deepak.prajapat@poornima.edu.in (D.K.P.); saurabh.singh@poornima.edu.in (S.S.)
² Civil Engineering Department, Malaviya National Institute of Technology, Jaipur 302017, India; mah_thory@yahoo.co.in
³ Faculty of Environmental Earth Science, Hokkaido University, Sapporo 060-0808, Japan
⁴ Department of Civil Engineering, Chennai Institute of Technology, Chennai 600069, India
⁵ Architecture and Planning Department, College of Engineering, King Khalid University, Abha 61421, Saudi Arabia; s.alsulamy@kku.edu.sa
⁶ Advanced Systems Analysis Group, International Institute for Applied Systems Analysis, Schlossplatz 1, A-2361 Laxenburg, Austria; kharrazi@iiasa.ac.at
⁷ Network for Education and Research on Peace and Sustainability (NERPS), Hiroshima University, Hiroshima 739-0046, Japan
* Correspondence: ram@ees.hokudai.ac.jp

Abstract: With global temperatures steadily rising, understanding the impacts of warming on regional climates has become crucial, particularly for countries like India, where climate sensitivity has significant socio-economic implications. This study assesses the trends and spatial distribution of summer days across India under different warming targets (1.5 °C, 2 °C, 2.5 °C, 3 °C, 3.5 °C, 4 °C, 4.5 °C, and 5 °C) and emission scenarios (RCP4.5 and RCP8.5). A Multi-Model Ensemble (MME) approach, combining five best-performing CORDEX-SA experiments, was utilized to analyze projected summer days in India. Non-parametric trend analysis techniques—such as the Mann–Kendall test, Modified Mann–Kendall, Sen’s Slope estimator, and Pettitt test—were used to investigate temporal patterns, and Reliability Ensemble Averaging (REA) was applied for uncertainty analysis to ensure robust projections. The results indicate that summer days are expected to increase significantly across India under both RCP scenarios, with the highest increases projected for northeastern regions and north-central regions of India. This study underscores the pressing need for region-specific adaptation strategies to manage extended periods of extreme temperatures and safeguard public health, agriculture, and socio-economic stability.

Keywords: global warming; summer days; India; RCP4.5; RCP8.5; climate change; CORDEX-SA; Multi-Model Ensemble; adaptation strategies; heat stress



Academic Editor: Charles Jones

Received: 27 February 2025

Revised: 27 April 2025

Accepted: 29 April 2025

Published: 13 May 2025

Citation: Prajapat, D.K.; Choudhary, M.; Avtar, R.; Singh, S.; Alsulamy, S.; Kharrazi, A. Transformative Spatio-Temporal Insights into Indian Summer Days for Advancing Climate Resilience and Regional Adaptation in India. *Earth* **2025**, *6*, 39. <https://doi.org/10.3390/earth6020039>

Copyright: © 2025 by the authors. Licensee MDPI, Basel, Switzerland. This article is an open access article distributed under the terms and conditions of the Creative Commons Attribution (CC BY) license (<https://creativecommons.org/licenses/by/4.0/>).

1. Introduction

With global temperatures steadily rising, understanding the impacts of warming on regional climates has become crucial, particularly for countries like India, where climate sensitivity has significant socio-economic implications. This study assesses the spatial and temporal variations of summer days across India under different warming targets and emission scenarios (RCP4.5 and RCP8.5). While various heat stress indicators such as the Heatwave Duration Index (HWDI), maximum temperature percentiles (TX90p), or Wet

Bulb Temperature (WBT) exist, this study utilizes the “Summer Days” (SU) index, defined as the number of days with daily maximum temperature (Tmax) exceeding 30 °C. This threshold is adopted from the India Meteorological Department (IMD), making it a locally relevant and policy-aligned indicator for monitoring moderate heat stress. It provides a clear, interpretable metric for assessing prolonged warm conditions that are critical for sectors like agriculture, public health, and energy planning. A Multi-Model Ensemble (MME) approach, using an ensemble of five best-performing CORDEX-SA experiments, was utilized to analyze projected summer days in India. Different non-parametric trend analysis techniques were employed to investigate spatial and temporal changes, and Reliability Ensemble Averaging (REA) was applied for uncertainty analysis to ensure robust projections.

Climate change has emerged as one of the most pressing issues of our time [1], significantly impacting global and regional temperature patterns, precipitation regimes, and the occurrence of extreme weather events [2,3]. Over the past few decades, several studies have documented the wide-ranging consequences of climate change, emphasizing the importance of understanding its impacts at both the global and local scales [4–6]. Specifically, regional temperature patterns and changes in extreme temperature events, such as heatwaves and cold spells, are crucial for assessing the risks associated with climate change, particularly for a densely populated and climate-sensitive country like India [7].

With global temperatures on the rise, the frequency and duration of summer days are expected to increase, amplifying vulnerabilities across India’s critical sectors. Figure 1 shows the multidimensional impacts of rising summer days on public health, agriculture, infrastructure, water resources, and urban environments. These impacts include increased heat-related illnesses and mortality, decreased crop productivity, elevated irrigation demands, and intensification of the urban heat island (UHI) effect. The projected escalation in summer days poses a direct threat to climate-sensitive populations, ecosystems, and economic stability, necessitating urgent region-specific adaptation strategies.

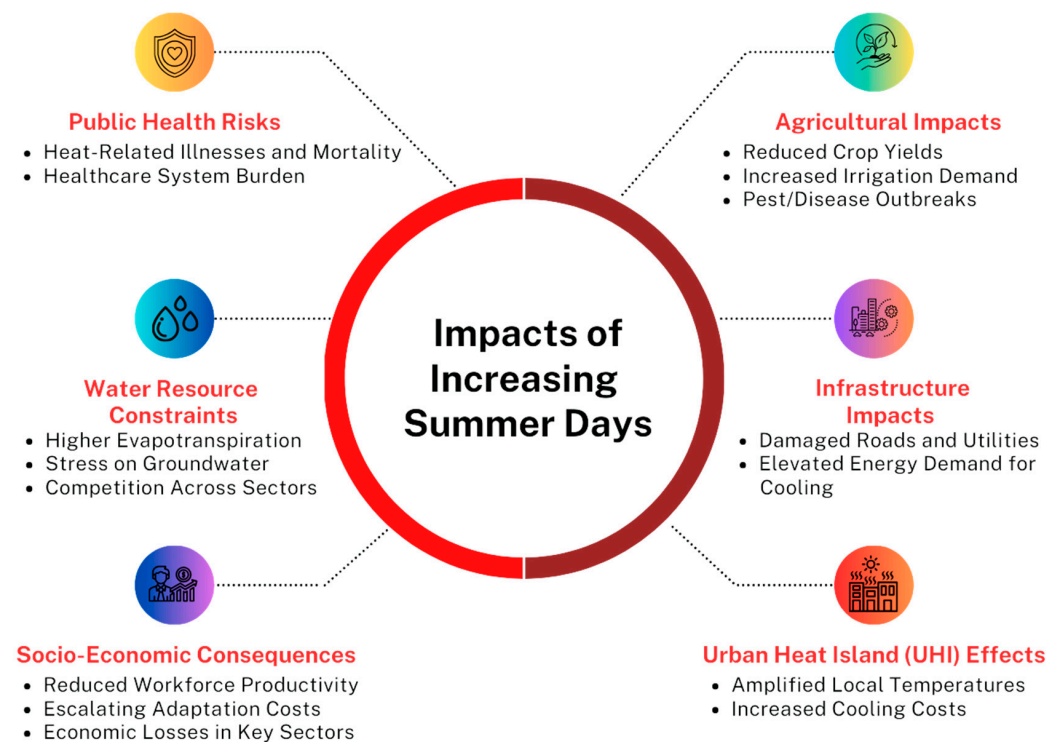


Figure 1. Impacts of increasing summer days on various sectors [8–10].

In recent years, downscaling experiments such as the Coordinated Regional Climate Downscaling Experiment for South Asia (CORDEX-SA) have provided significant insights into regional climate change projections [11]. The CORDEX-SA simulations have been instrumental in delivering high-resolution climate projections that can be used to assess the impacts of climate change at the regional level [12]. Singh and Patwardhan (2012) observed an increasing trend in extreme weather events like floods and heatwaves across India, emphasizing the importance of robust data collection and research to address these challenges [13]. Lastly, Paul and Maity (2023) analyzed climate extremes in Northeast India and Bangladesh, predicting substantial temperature increases and more frequent heavy precipitation days by the century's end under high-emission scenarios, underscoring the necessity for regional planning to mitigate impacts on agriculture and water resources [14]. Understanding the behaviour of summer days under different warming scenarios is crucial, as such information can guide adaptation strategies in agriculture, water resource management, and public health [15,16]. In their respective studies, Yaduvanshi et al. (2019) analyzed the impact of 1.5 °C and 2 °C global warming on regional temperature and rainfall across India, noting significant increases in rainfall, especially in northeastern and southern regions, and greater temperature rises in northern states [17]. Maharana (2024) projected an increase in rainfall for Odisha, predicting more frequent and intense rainfall events that could extend the rainy season and heighten flood and drought risks [18]. Li et al. (2022) focused on global maize production under similar warming scenarios, forecasting a significant yield reduction, especially under the 2 °C scenario, with associated economic impacts [19]. Bai et al. (2023) explored how land use and meteorological changes under different climate scenarios could affect regional climates, such as in Zhengzhou, China, revealing that such changes could substantially alter temperature and precipitation patterns [20]. Huang et al. (2017) investigated the impacts of global warming on different types of droughts in the U.S., forecasting an increase in agricultural and hydrological droughts with rising global temperatures [21]. Chauhan et al. (2022) studied rainfall variability in Haryana from 1901 to 2020, noting significant spatio-temporal differences and trends suggesting climate-induced changes in rainfall patterns [22]. T, AchutaRao, and Sagar (2023) projected an intensification and prolongation of heatwaves in India under 1.5 °C and 2.0 °C warming scenarios, highlighting the enhanced health risks during the humid monsoon season and the need for advanced adaptation strategies [23]. Despite significant research on global warming impacts, a detailed understanding of the spatio-temporal variations of extreme temperature events like summer days across India's diverse climatic zones remains limited. Existing studies often do not provide sufficiently localized data to effectively guide adaptation strategies for heat-related health risks and agricultural productivity. Additionally, there is a lack of integration between climatic impact assessments and socio-economic factors, which is crucial for addressing potential risks to agriculture, health, and infrastructure effectively. This gap impedes the formulation of comprehensive, region-specific climate resilience strategies essential for India's climate-sensitive sectors.

This study aims to contribute to a more comprehensive understanding of future climate risks in India, aiding policymakers and stakeholders in their climate resilience efforts.

The primary objective of this study is to assess the spatio-temporal variations in summer days across India under different warming targets (1.5 °C, 2 °C, 3 °C, etc.) and emission scenarios (RCP4.5 and RCP8.5). This is highly significant, as it addresses the regional climate impacts that are essential for understanding the potential risks to agriculture, health, and infrastructure. Given India's socio-economic reliance on climate-sensitive sectors, understanding how summer days might evolve under global warming helps in creating informed, adaptive strategies to protect vulnerable populations and ensure sustainability in critical sectors.

This study's novelty lies in its focus on summer days as a key indicator of heat stress and its use of Reliability Ensemble Averaging (REA) to enhance projection accuracy. Unlike prior research, which often focuses on broader climate impacts, this work emphasizes the effects of prolonged moderately high temperatures, providing crucial insights into regional heat stress and socio-economic consequences. The REA approach reduces uncertainties more effectively than traditional ensemble methods by weighting models based on historical performance, resulting in more reliable climate projections.

The significance of this work lies in its contribution to region-specific adaptation strategies for mitigating the impacts of increased summer days. By providing detailed and reliable projections, this study helps inform policymakers and stakeholders about potential risks, enabling better planning for public health, agriculture, and socio-economic stability in India.

2. Materials and Methods

2.1. Indian Warming Targets (IWTs) and Climate Models

This study evaluates the impacts of temperature rise on summer days across India, utilizing multiple CORDEX-SA (Coordinated Regional Climate Downscaling Experiment for South Asia) experiments under two representative emission scenarios, RCP4.5 and RCP8.5. The RCP4.5 represents the current emission scenario, and RCP8.5 is an extreme/high emission scenario. These scenarios are most widely used in regional climate change studies. There is another scenario RCP2.6, but it is not included in this study because it is an extremely ambitious mitigation scenario that requires negative emissions. The current emissions trajectories make it increasingly implausible. So, only RCP4.5 AND RCP8.5 scenarios are used in this study. Climate models are crucial for predicting future climate scenarios and understanding complex climate interactions and variability. The CORDEX-SA experiments provide high-resolution (~50 km) regional climate projections, which are essential for assessing the impacts of climate change at a regional level. All experiments were originally available at a horizontal resolution of approximately 0.44° (~50 km). To ensure consistency in spatial analysis, we conducted spatial homogenization by interpolating all model outputs onto a common regular grid using Climate Data Operators (CDO). This step allowed for uniform spatial comparison across the Indian domain.

The selection of CORDEX-SA models was based on several criteria to ensure the robustness and reliability of the projections. The primary criteria included the ability of models to replicate historical climate patterns accurately, mainly focusing on maximum temperature data from 1981 to 2005. Model outputs were compared against observed data from the India Meteorological Department (IMD). Models demonstrating high correlation and minimal deviation from observed data were prioritized.

In addition, the spatial resolution and completeness of the models were also considered. Models with higher spatial resolution and comprehensive temporal coverage over the Indian subcontinent were prioritized to ensure an effective representation of climate variability across different regions. Another critical criterion was the physical consistency of the models, specifically, their ability to simulate known climatic processes across the diverse climatic zones of India, including the onset, withdrawal, and distribution of the monsoon, which significantly influences temperature extremes in India. Table 1 presents the details of the CORDEX-SA experiments analyzed in this study. Each experiment consisted of a Regional Climate Model (RCM) driven by a corresponding Coupled Model Intercomparison Project Phase 5 (CMIP5) Global Climate Model (GCM).

Table 1. Details of CORDEX-SA experiments analyzed in the present study (source: CORDEX South-Asia Database, CCCR, IITM; <http://cccr.tropmet.res.in/cordex/files/downloads.jsp>, 20 December 2024).

S.N.	Experiment Name	Name Used in This Study	CORDEX South Asia RCM	Driving CMIP5 GCM
1	CCCma-CanESM2- IITM-RegCM4	CanESM2		CCCma-CanESM2
2	GFDL-ESM2M-IITM-RegCM4	GFDL	IITM-RegCM4	NOAA-GFDL-GFDL-ESM2M
3	IPSL-CM5A-LR-IITM-RegCM4	IPSL		IPSL-CM5A-LR
4	CSIRO-Mk3.6.0-IITM-RegCM4	CSIRO		CSIRO-Mk3.6.0
5	MIROC-MIROC5- SMHI-RCA4	MIROC		MIROC-MIROC5
6	CNRM-CM5-SMHI-RCA4	CNRM		CNRM-CM5
7	MOHC-HadGEM2-ES-SMHI-RCA4	HadGEM	SMHI-RCA4	MOHC-HadGEM2-ES
8	NCC-NorESM1-M-SMHI-RCA4	NorESM		NCC-NorESM1-M
9	MPI-ESM-LR-REMO2009	MPI	MPI-CSC-REMP2009	MPI-ESM-LR

The selected models underwent rigorous validation to assess their reliability in capturing climate variability at regional scales. This validation involved statistical cross-validation techniques, where historical data were divided into training and validation sets to test the predictive accuracy of each model. Key performance metrics included Pearson correlation coefficients, root mean square error (RMSE), and mean bias. The Pearson correlation coefficient was used to evaluate the linear relationship between model outputs and observed data, while RMSE assessed the average magnitude of errors, and mean bias represented the average difference between predicted and observed values. These metrics were essential for determining each model’s capability to capture both the mean state and variability of historical climate conditions.

Based on their superior performance in reproducing historical climate patterns—particularly, maximum temperature trends, seasonal consistency, and low statistical bias—five CORDEX-SA experiments were selected for Multi-Model Ensemble (MME) analysis. These top-performing models, along with their evaluation criteria, are summarized in Table 2. To evaluate climate impacts under progressive warming, the concept of Indian Warming Targets (IWTs) was adopted, referring to global mean surface temperature increases of 1.5 °C, 2.0 °C, 2.5 °C, 3.0 °C, 3.5 °C, 4.0 °C, 4.5 °C, and 5.0 °C above pre-industrial levels. These warming thresholds were linked to model outputs through the calculation of Threshold Crossing Times (TCTs), which represent the period when the 21-year moving average of annual mean temperature exceeds a specific warming level relative to the baseline (1981–2005).

Table 2. Summary of selected CORDEX-SA experiments used in MME based on model performance.

S.N.	Model Code	Driving GCM	Key Performance Criteria	MPI Rank
1	CanESM2	CCCma-CanESM2	High Tmax correlation with IMD; low bias	Top 5
2	GFDL	NOAA-GFDL-ESM2M	Strong seasonal monsoon simulation	Top 5
3	CSIRO	CSIRO-Mk3.6.0	Accurate in North India, low RMSE	Top 5
4	MIROC	MIROC5	Good temporal consistency	Top 5
5	IPSL	IPSL-CM5A-LR	Low mean bias, consistent interannual variability	Top 5

Once the TCT was determined for each IWT level, the corresponding 30-year climate window centered around the TCT was used to extract model data and analyze summer day projections. This method ensures that the climate indicators are evaluated relative to warming intensity, rather than fixed time periods, enabling a more policy-relevant,

temperature-aligned analysis of climate risks. To link the IWTs with model outputs, we adopted a temperature-aligned analysis approach. For each CORDEX-SA experiment, the time series of annual mean surface air temperature was smoothed using a 21-year moving average. The year when this smoothed average first crossed a specific IWT level (e.g., 1.5 °C, 2 °C, etc.) relative to the baseline (1981–2005) was defined as the Threshold Crossing Time (TCT). A centered 30-year window around each TCT was then selected to extract model data for that particular warming level. This methodology ensures that climate indicators such as summer days are evaluated not by fixed time periods (e.g., mid-century), but by warming intensity, which offers a more policy-relevant, impact-aligned assessment framework.

2.2. Bias Correction and Model Performance Evaluation

Due to inherent biases in climate models, a delta bias correction approach was applied to align model outputs with observed historical data more closely, thus enhancing the reliability of future climate projections. The bias correction process began with bias detection, where model outputs from the historical period (1981–2005) were compared against observational data. The bias was calculated using the formula:

$$\text{Bias} = \frac{\sum(P_i - O_i)}{n}$$

where P_i represents the predicted values, O_i represents the observed values, and n is the number of data points.

Once the bias was detected, the delta correction approach involved subtracting the calculated bias (delta) from the model’s projected values for future scenarios. This ensured that the corrected model output was aligned more closely with historical observations, providing more reliable projections.

To validate the effectiveness of the bias correction, corrected model outputs were compared against independent datasets not used in the bias detection process. This comparison was critical to confirm that the bias correction resulted in outputs that more accurately represented actual climatic conditions.

After bias correction, the Model Performance Index (MPI) was used to evaluate and rank the models based on their improved accuracy. MPI was calculated using multiple statistical metrics, such as Pearson correlation, RMSE, and bias. Table 3 provides the formulas used to calculate these metrics, which were used to assess the performance of each model.

Table 3. Formulas used in model performance evaluation.

Metric	Formula	Description
Pearson Correlation	$r = \frac{\sum(X-\bar{X})(Y-\bar{Y})}{\sqrt{\sum(X-\bar{X})^2\sum(Y-\bar{Y})^2}}$	Measures the linear correlation between the model and observed data
Root Mean Square Error	$\text{RMSE} = \sqrt{\frac{\sum(P_i - O_i)^2}{n}}$	Measures the average magnitude of the errors between predictions (P) and observations (O)
Bias	$\text{Bias} = \frac{\sum(P_i - O_i)}{n}$	Measures the average difference between predictions and observations

The MPI score for each model was computed, and the models were ranked accordingly. The top-performing models were then selected for the analysis of future climate projections. The MME was calculated after using the five best-performing CORDEX-SA ex-

periments for Indian region. The MME ensemble was calculated as average of CORDEX-SA experiment data.

2.3. Analysis of Extreme Temperature Indices (ETIs)

A detailed spatial and temporal analysis of summer days (SU) was conducted using the best-performing, bias-corrected models under RCP4.5 and RCP8.5 scenarios. As per the Indian Meteorological Department (IMD) climate indices, a “summer day” is defined as a day when the daily maximum temperature exceeds 30 °C. This threshold was used to identify summer days across India.

Although the SU index considers only maximum temperature thresholds, it remains one of the most policy-relevant and widely understood metrics in climate risk assessments. It directly reflects human exposure to prolonged heat, and indirectly captures heat stress impacts across agriculture, urban infrastructure, and public health sectors. While alternative indices—such as apparent temperature or the heat index—may better represent the combined effects of temperature and humidity, reliable humidity projections at the regional scale remain limited under current CORDEX-SA outputs. Therefore, SU serves as a consistent, data-driven, and actionable proxy for assessing rising heat stress conditions in India.

The analysis focused on evaluating the variation in the frequency of summer days across India and their temporal evolution under different Indian Warming Targets (IWTs). Additionally, the Threshold Crossing Time (TCT) was analyzed to determine when specific warming thresholds were exceeded across the study area.

While it is acknowledged that the SU index alone does not fully capture the multi-dimensional nature of heat stress—particularly the role of relative humidity—this study prioritizes SU due to its standardized definition, strong policy relevance, and consistent availability across CORDEX-SA outputs. Humidity-based indices such as the Heat Index (HI) or Wet Bulb Temperature (WBT) require high-resolution humidity data, which is not currently available at the required temporal and spatial resolution. Future studies may build upon this work by incorporating such indices as more reliable regional datasets become available.

2.4. Reliability Ensemble Averaging (REA) for Uncertainty Analysis

To quantify and reduce uncertainty in model projections, the Reliability Ensemble Averaging (REA) method was applied. REA provides a mechanism for combining results from different models while assigning weights to each model based on its performance and convergence with observational data. The REA weight (w_i) for each model (i) is calculated using the formula:

$$w_i = \frac{1}{\sigma_i^2}$$

where σ_i represents the model’s uncertainty. By applying the REA method, the uncertainties in ensemble projections were minimized, resulting in more robust and reliable climate forecasts for summer days across India under different IWTs.

This comprehensive methodology provides transparency in model selection, bias correction, and validation, ensuring that the resulting projections are both robust and reliable. By addressing the reviewers’ concerns, this detailed explanation demonstrates the strength of the model selection, validation, and bias correction processes used in this study.

3. Results

3.1. Spatial Distribution of Summer Days (SU) Projected by MME Under RCP4.5 Scenario

Spatial distribution of annual mean summer days (SU) during the historical period (1981–2005) and its future projections under different IWTs under RCP4.5 is shown in Figure 2. Evaluation data show that the annual mean SU of India was 260.10 days, which spatially varied between 0 and 365 days in India during the historical period. The MME mean simulates 260.11 days, which spatially varied between 0 and 365 days in India. Western Himalaya and some parts of North-East India do not have any summer days in a year during this period. It was minimum in the foothills of Himalaya and increased gradually towards southern regions of India (East Coast, West Coast, and Peninsular India). In East Coast and West Coast India, the daily maximum temperature is higher than 25 °C throughout the year. Annual mean changes in SU under 1.5–2.5 °C IWT are also shown in Figure 2 for the RCP4.5 scenario. The MME projection shows all India annual mean SU will increase by 15.13 days under warming of 1.5 °C, and this increase will spatially vary between 0 days and 31.01 days in India. It is projected to increase with an average of 18.85 days (spatially vary: 0 to 43.50 days) due to 2 °C IWT under this scenario. If the mean warming in India crosses the 2.5 °C IWT, annual mean SU will increase with an average of 21.98 days, which spatially varies between 0 and 52.62 days in India. The MME simulates that the maximum rise in SU will be in North-Central and North-East India, followed by North-West India. East Coast and West Coast regions have SU throughout the year, so changes are zero in these regions. The annual mean SU will increase spatially between 35 and 52.60 days in North-Central and North-East India due to 2.5 °C IWT of this scenario. A mean yearly rise of 20 to 35 days will occur in North-West India, while in the Interior peninsula and Coastal region, it will be less than 25 days during this WT. The inner areas of the central peninsula will get a higher rise of SU as compared to outer regions.

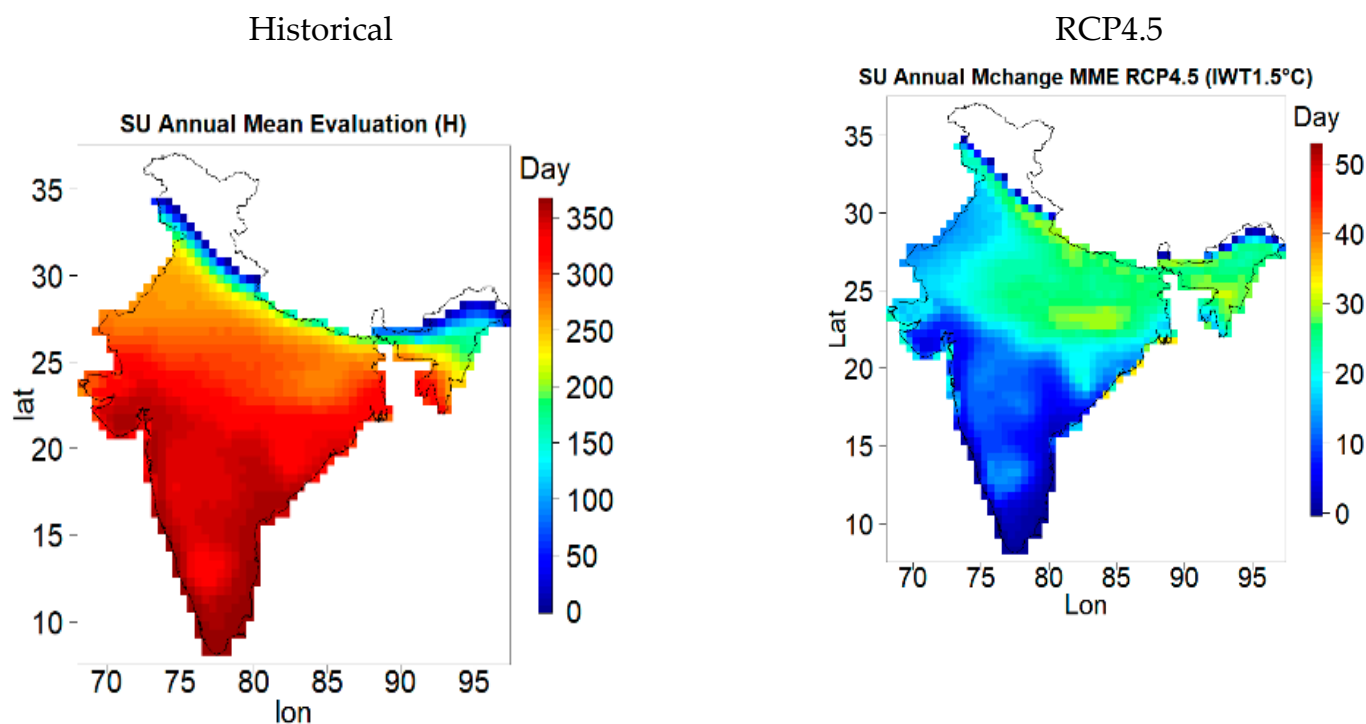


Figure 2. Cont.

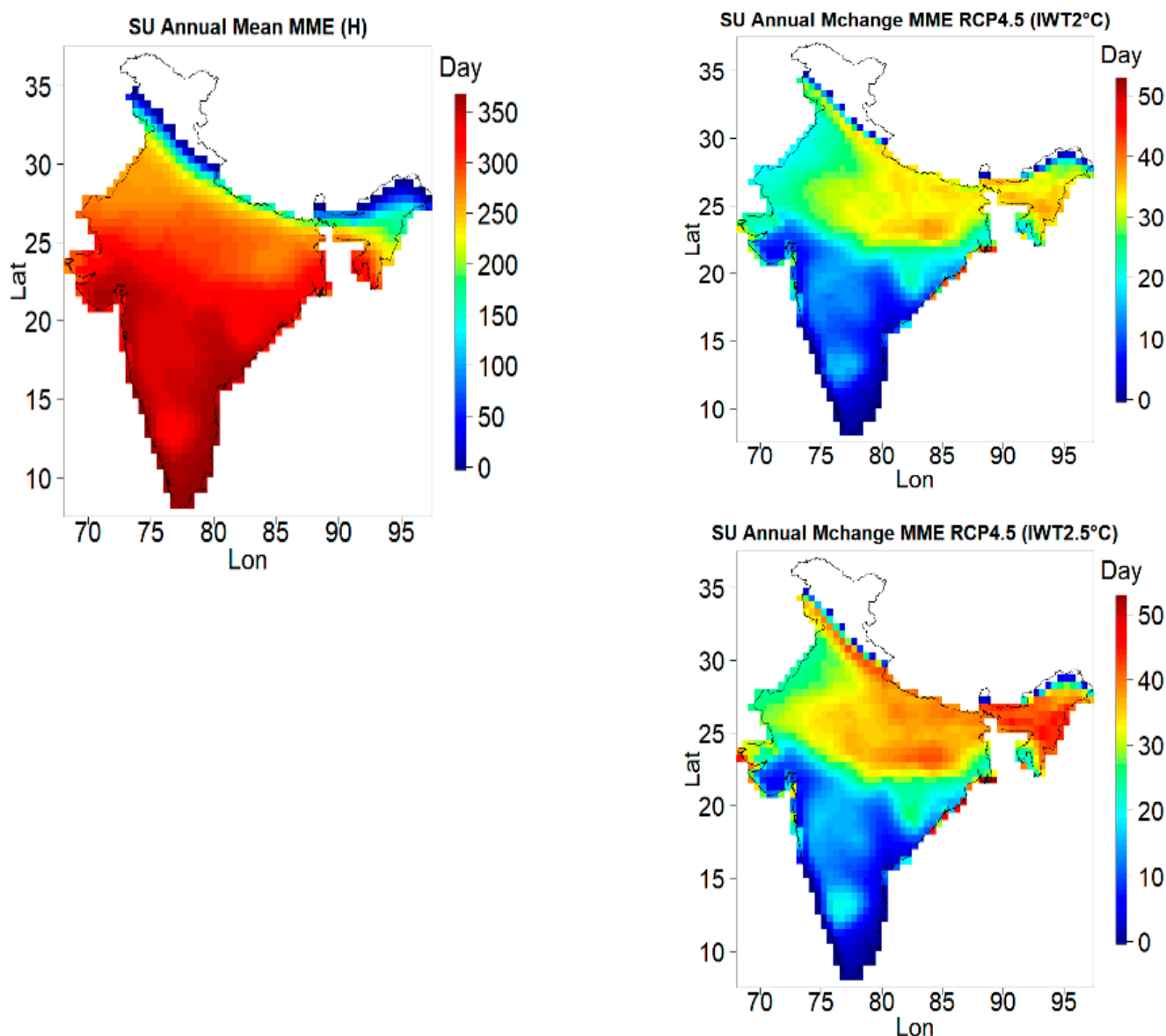


Figure 2. Spatial distribution of annual mean frequency of summer days during the historical period (1981–2005) by evaluation data and MME (**Left column**) and relative changes under Indian Warming Targets (IWTs) of RCP4.5 (1.5–2.5 °C) (**Right column**).

3.2. Spatial Distribution of Summer Days (SU) Projected by MME Under Rcp8.5 Scenario

Spatial distribution of annual mean summer days (SU) during the historical period (1981–2005) and its future projections under different IWTs under RCP8.5 is shown in Figure 3. Annual mean SU is increasing relative to the historical period, and it will continue to increase due to the occurrence of high warming targets in the 21st century. Figure 3 represents the mean spatial variation in annual SU due to 1.5–4.5 °C IWT under the RCP8.5 scenario. The MME mean simulates 260.11 days, which spatially varied between 0 and 365 days in India. Western Himalaya and some parts of North-East India do not have any summer days in a year during this period. It was minimum in foothills of Himalaya and increased gradually towards southern regions of India (East Coast, West Coast, and Peninsular India). In East-Coast and West Coast India, the daily maximum temperature is higher than 25 °C throughout the year.

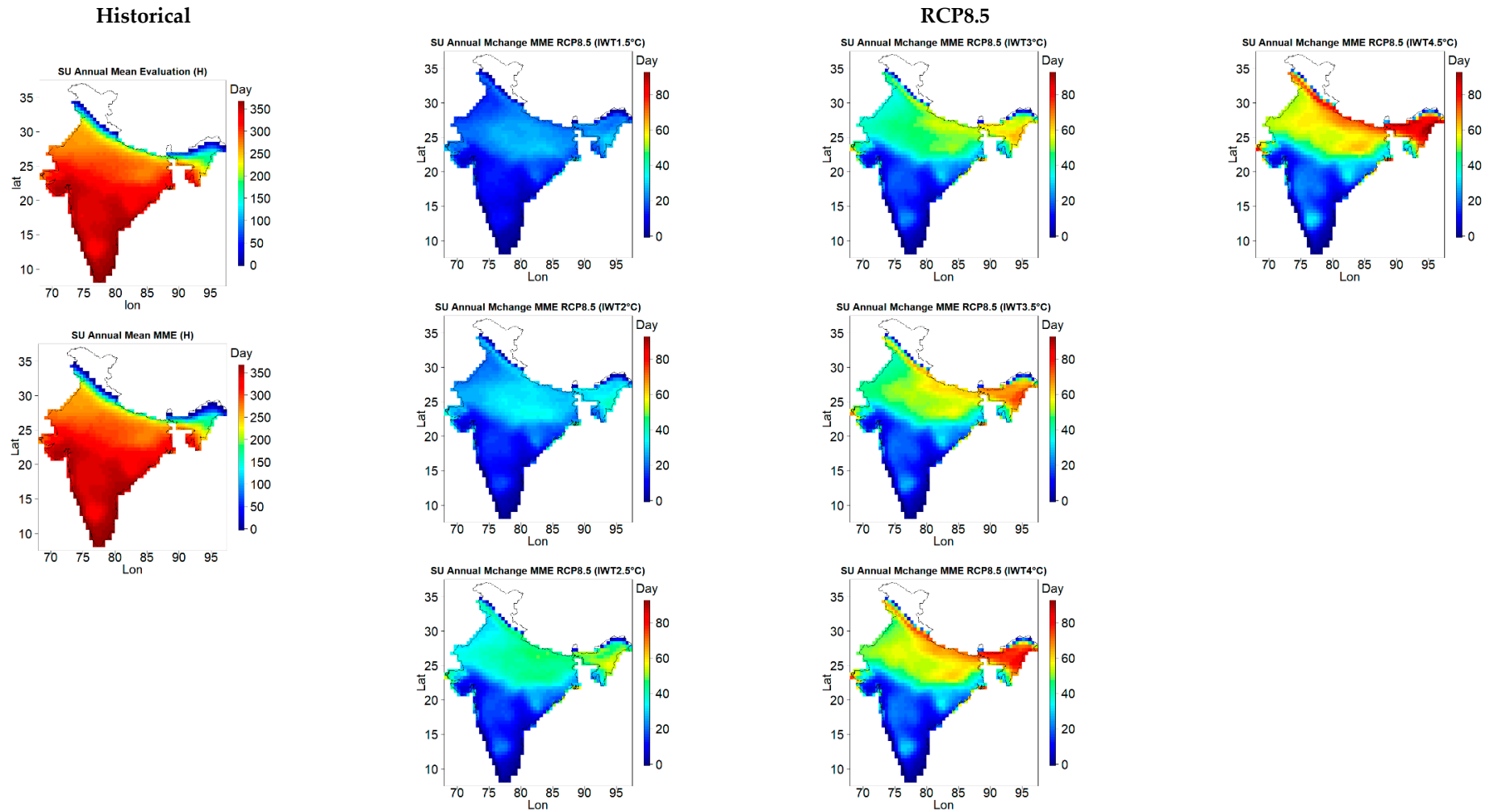


Figure 3. Spatial distribution of annual mean frequency of summer days during the historical period (1981–2005) by evaluation data and MME and relative changes under Indian Warming Targets (IWTs) of RCP8.5 (1.5–4.5 °C).

It was found that the spatial distribution of mean changes remains the same in both RCPs; only the magnitude of mean changes varies with increasing WT and RCPs. Annual mean SU is simulated to increase with an average of 14.81 days per year due to 1.5 °C IWT by MME with spatial variation between 0 and 32.81 days in India under RCP8.5. It is projected to increase by 18.81 days (spatially vary: 0 to 43.78 days) per year due to 2 °C WT of India. In India, the warming will become more intense, which will cause a rise of mean SU with 25.20, 28.21, 31.48, and 34.22 days due to 2.5, 3, 3.5, and 4 °C IWT under this scenario. It will increase by 36.04 days (spatially vary: 0 to 92.02 days) due to extreme IWT 4.5 °C of RCP8.5. The North-East region will be the most affected region for the mean rise in SU under this scenario. In this region, it will increase by more than 80 days for 4.5 °C IWT. The foothills of Himalayas also show significantly increasing SU. The annual mean rise of SU will vary between 50 and 70 days in North-Central India, while in the Interior peninsula and Coastal regions, it will increase up to 40 days per year due to 4.5 °C IWT of RCP8.5 scenario.

The result represents that the rise in summer days is predominantly in Northern India under both scenarios. There are multiple reasons behind the rising of SD in this region. During summer, the strong high-pressure system over the Tibetan Plateau causes air to subside over Northern India. This subsidence creates compressional heating and suppresses cloud formation, leading to clearer skies and more intense solar heating. The hot and dry winds from the Thar Desert transport heat eastward across the northern plains. These winds, sometimes called “loo”, can raise temperatures by 5–8 °C above normal. Northern India’s dense urban areas (Delhi, Lucknow, etc.) with extensive concrete surfaces exacerbate heating through the urban heat island effect, making temperature increases more pronounced than in rural areas. These atmospheric processes combine to make Northern India particularly vulnerable to increasing summer days under climate change scenarios.

3.3. Trend Analysis for Annual Mean Summer Days Projected by MME and CORDEX-SA Experiments

Time series of all India annual mean Summer Days (per grid) projected by evaluation data and four CORDEX-SA experiments with their MME are shown in Figure 4a–c for the historical period (1981–2005) and long-term climatology (2006–2099) under RCP4.5 and RCP8.5 scenarios. Trend analysis statistics for evaluation data and all experiments are given in Table 4, with MME projections under different IWTs of both RCPs. These statistical properties are obtained from trend analysis using MK (Mann–Kendall) or Modified MK (Z or Zc) and Sen’s Slope estimator test for annual time series. Trend statistics Z or Zc values represent the positive or negative trends in the time series. The P or Pc values represent the significance of the trend at a 5% significance level ($P/P_c \leq 0.05$). The Sen’s Slope (SS) estimator test represents the magnitude of the trend per decade. Pettitt *t*-test statistics show the major change point/year in the time series. Summer days are simulated to increase significantly ($Z/Z_c = 3.77$; $P/P_c = 0.00$) with a rate of 2.98 days per decade by evaluation data during the historical period. The MME also shows a significantly increasing trend ($Z/Z_c = 4.93$; $P/P_c = 0$) during this period, with a rate of 4.28 days per decade. MME projections for long-term climatology indicate that it will increase significantly under both RCPs. During this period, it will increase with a rate of 1.99 days per decade and 3.89 days per decade under RCP4.5 and RCP8.5 scenarios, respectively. It will also increase significantly during all WTs of both scenarios. It will increase by 4.17 days per decade and 4.32 days per decade during the 1.5 °C WT of RCP4.5 and RCP8.5 scenarios, respectively. The Sen’s Slope is found to be maximum for 1.5 °C (4.17 days per decade) of RCP4.5 and 2.5 °C WT (5.39 days per decade) of the RCP8.5 scenario. The Sen’s Slope is projected to be 3.11 days per decade for 2 °C and 1.25 days per decade for 2.5 °C WT of RCP4.5. It is projected to decrease from lower to higher WTs under the RCP4.5 scenario. The major

changing year from the Pettitt *t*-test was simulated to be 1984 and 1996 by evaluation data and MME. The MME projects that these changing years will be 2042 and 2052 during the long-term climatology of RCP4.5 and RCP8.5, respectively. It will be 2030 and 2024 during the 1.5 °C WT of RCP4.5 and RCP8.5 scenarios, respectively. Trend analysis for time series from all experiments represents a significant rising trend, except the MPI experiment, which has an insignificant rising trend during the historical period. The Sen’s Slope simulated by these experiments varies between 2.54 and 4.49 days per decade. The changing year varied between 1992 and 1999 during this period. The Sen’s Slope projected by GFDL is maximum and minimum by MPI experiments during the historical period. All experiments have a significant increasing trend during long-term climatology under RCP4.5, and the trend statistics vary between $Z/Z_c = 7.40$ and 9.45 , $P/P_c = 0.00$, and Sen’s slope = 1.53 days per decade to 1.99 days per decade. It will also increase significantly under RCP8.5, with a rate varying between 3.21 and 4.24 days per decade. All experiments will have a significant increasing trend under most of the IWTs of both RCPs. The significant changing years are projected by all experiments between 2041–2051 and 2050–2054 under RCP4.5 and RCP8.5 for long-term climatology, respectively. The detailed trend analysis statistics for all experiments under IWTs are given in Table 3 below.

It is essential to quantify the uncertainty in the annual frequency of extreme temperature indices due to the presence of bias in future climate projections from climate models. The Reliability Ensemble Averaging (REA) technique is used to assess the uncertainty in the annual mean frequency of each extreme index under different IWTs of the RCP4.5 and RCP8.5 scenarios. Table 5 presents the relative changes (from the historical period) in annual mean frequency projected by the MME with its uncertainty under RCP4.5 and RCP8.5 emission scenarios. The annual mean of SU was simulated to be 260.10 days by evaluation and MME during the historical period. During the warming of 1.5 °C and 2 °C over India, it will increase by 15.13 ± 2.52 days (14.81 ± 1.9 days) and 18.85 ± 2.30 days (18.81 ± 2.20 days) under RCP4.5 (RCP8.5) scenarios, respectively. The uncertainty varies between 2.30 and 2.57 days and 1.9 and 4.50 days during all IWTs of RCP4.5 and RCP8.5 scenarios, respectively.

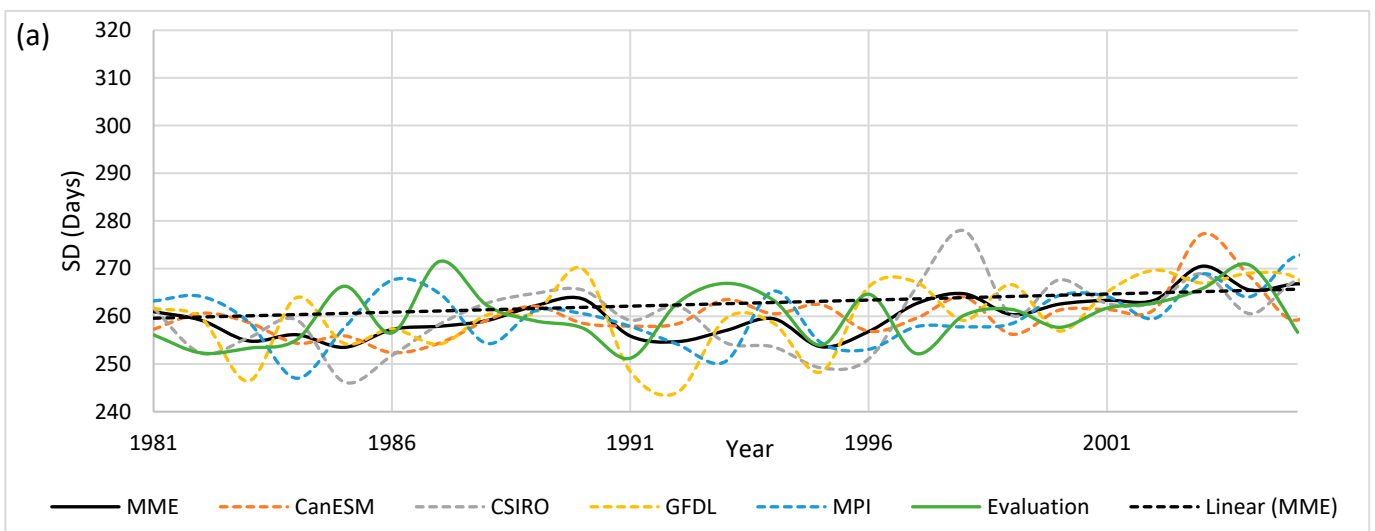


Figure 4. Cont.

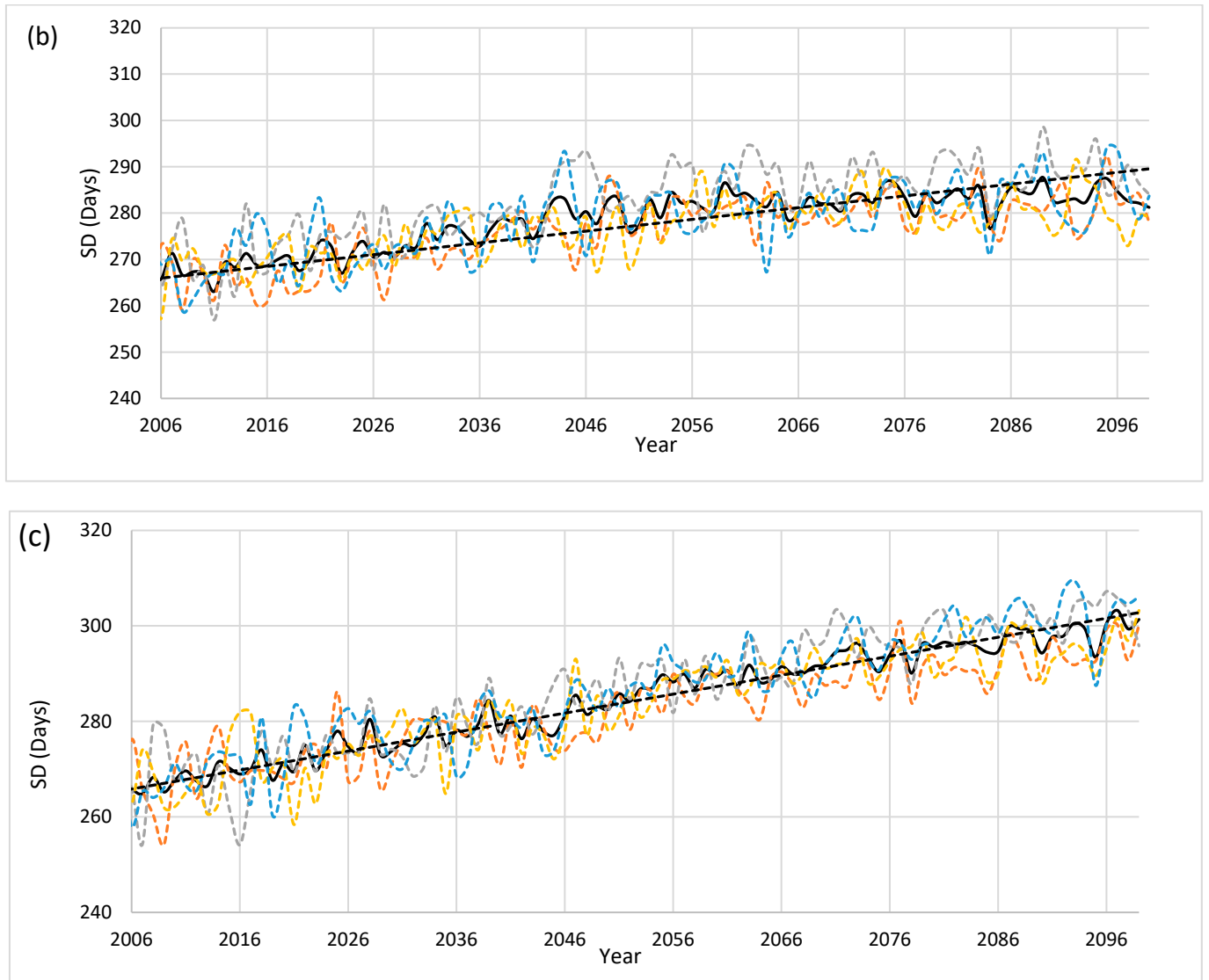


Figure 4. Time series of annual mean summer days (per grid; total grids 1297) during (a) historical period (1981–2005), (b) RCP4.5 (2006–2099), and (c) RCP8.5 (2006–2099) projected by evaluation, MME, and four CORDEX-SA experiments.

Table 5. Annual mean statistics of summer days projected by MME in the historical period (1981–2005) and relative changes during IWTs with its uncertainty under RCP4.5 and RCP8.5 emission scenarios.

ETI	Historical	RCP4.5			RCP8.5						
		1.5 °C	2 °C	2.5 °C	1.5 °C	2 °C	2.5 °C	3 °C	3.5 °C	4 °C	4.5 °C
SU	260.10 (260.10)	15.13 ± 2.52	18.85 ± 2.30	21.99 ± 2.57	14.81 ± 1.9	18.81 ± 2.20	25.20 ± 2.60	28.21 ± 3.80	31.48 ± 4.41	34.22 ± 4.23	36.04 ± 4.50

Note: Historical values in bracket () are for evaluation data.

4. Discussion

The findings of this study provide critical insights into the increasing frequency of summer days across India under different warming scenarios, highlighting significant spatial and temporal variations. Regions such as North-Central and North-East India are projected to see the largest increases, while coastal areas are expected to experience consistently high temperatures. This variation underscores the need for targeted adaptation measures, distinguishing this work from prior studies that often lacked detailed regional analysis. Additionally, different studies can show the different rate of warming due to utilization of different types of climate models at different resolution. So, the regional impact can be different than the mean warming of the country or globe. The regional warming rates are also different for different regions of country due to the combined effects of seasonal aerosol loading and intensive irrigation practices in such regions.

The projected increase in summer days varies significantly across regions, with some areas facing disproportionately higher risks. For example, parts of North-Central India, including eastern Uttar Pradesh and Bihar, are projected to experience an increase of over 50 summer days under a 4 °C warming scenario. These regions are not only densely populated, but also highly dependent on subsistence agriculture, increasing their vulnerability to heat-related crop failures and water stress.

In the Northeast, states like Assam and Meghalaya show a rising trend in summer days. When combined with high ambient humidity, even moderate temperature increases can elevate the risk of heat-related illnesses, especially among vulnerable populations. Meanwhile, urbanized regions of western India, including Delhi and Jaipur, are already impacted by the Urban Heat Island (UHI) effect, which is likely to intensify with the rise in Summer Days. This will exert added pressure on energy demand, cooling infrastructure, and public health systems.

These spatially differentiated patterns emphasize the urgency of implementing region-specific adaptation strategies that account for localized vulnerabilities and socio-economic dependencies.

These findings demonstrate that rising Summer Days are not just a linear function of time, but are strongly correlated with warming thresholds. By aligning the analysis with Indian Warming Targets (IWTs), this study provides an impact-oriented framework that is more intuitive and useful for policy planning. For example, the projected increase of 25–35 SU days under 2.5 °C warming in parts of North-Central India implies a near one-month extension of heat-related stress, which would substantially affect cropping cycles, increase water demand, and amplify public health burdens. Similarly, crossing the 4.5 °C threshold could mean over 80 additional SU days in the Northeast, stressing already fragile ecosystems and infrastructure. This temperature-aligned assessment helps align India's Nationally Determined Contributions (NDCs) and climate adaptation plans with scientifically grounded heat risk trajectories.

4.1. Broader Implications and Connection to Previous Studies

The observed rise in summer days is consistent with earlier research that identified an upward trend in extreme temperature events across South Asia. Unlike prior studies that focused on extreme heat or general temperature increases, this study explicitly examines summer days, providing a nuanced understanding of heat stress and its socio-economic impacts. The use of non-parametric statistical methods, such as the Mann–Kendall and Sen's Slope Estimator, revealed significant trends in summer days, especially under the RCP8.5 scenario, emphasizing the growing risks associated with unchecked emissions.

The use of Reliability Ensemble Averaging (REA) further differentiates this research by ensuring robust projections with minimized uncertainties, unlike traditional ensemble

averaging. This advanced approach provides a more accurate representation of future conditions, offering a valuable tool for effective climate adaptation planning.

4.2. Region-Specific Impacts and Adaptation Strategies

The summer days are going to have severe impacts in India in each field. Summer in India brings extreme heatwaves, leading to severe health risks. Prolonged exposure to high temperatures causes dehydration, heat exhaustion, and heatstroke, which can be fatal, especially for the elderly and children [24]. The Urban Heat Island (UHI) effect worsens conditions in cities, where concrete structures trap heat. The agricultural sector also suffers significantly during the Indian summer season. High temperatures and erratic rainfall reduce crop yields, particularly for wheat, pulses, and vegetables, leading to food inflation and farmer distress. Drought-like conditions force farmers to rely on expensive irrigation, increasing production costs. If the Summer Day will continue to increase, the livestock will also face heat stress and reduced milk production, which impacts rural incomes [8]. Water shortages become critical during peak summer months. Rivers, lakes, and groundwater levels deplete, leading to severe droughts in states like Maharashtra, Rajasthan, and Tamil Nadu. Major cities, including Chennai, Bengaluru, and Delhi, experience acute water crises, with tankers becoming the primary water source in some areas [9]. The rising Summer Days will lengthen the summer season so the demand for electricity soars as people rely heavily on air conditioners, coolers, and fans, leading to frequent power cuts and load shedding. Overburdened power grids struggle to meet consumption needs, affecting households and industries. Extreme heat also damages infrastructure: roads melt, railway tracks expand, and buildings develop cracks due to thermal stress. Summer heat also triggers forest fires, especially in Himalayan regions and dry deciduous forests, destroying wildlife habitats. The Himalayan glaciers melt at an accelerated rate, threatening long-term water security for northern India. Additionally, rising temperatures affect marine life, causing coral bleaching and disrupting aquatic ecosystems. To cope with extreme heat, daily routines shift, schools and offices adjust timings, and outdoor activities reduce. To combat these impacts, India is adopting measures like Heat Action Plans (HAPs) in cities, which include early warning systems, cooling shelters, and public awareness campaigns. Afforestation and urban greening help reduce the heat island effect. Government policies, such as subsidies for farmers and workers, aim to ease economic burdens [10].

The regional disparities in the projected increase in summer days necessitate targeted adaptation strategies. Public health measures, including Heat Action Plans (HAPs), cooling centers, and early warning systems, are particularly crucial for North-Central and North-East India, which are projected to see the highest temperature increases. Similarly, promoting heat-resilient crops and efficient water management practices is essential to sustain agriculture in these regions.

In urban areas along the East and West coasts, urban heat mitigation strategies—such as increasing green spaces, implementing cool roofing, and enhancing reflective surfaces—are necessary to combat the urban heat island effect. Strengthening energy infrastructure, including promoting energy-efficient cooling systems, is also crucial to managing the increased demand for cooling in urban regions.

4.3. Uncertainty Analysis and Policy Implications

The use of REA in this study demonstrates the value of reducing uncertainties by weighting models based on their historical performance, resulting in more reliable climate projections. Policymakers can utilize these reliable projections to formulate targeted adaptation strategies that address the unique vulnerabilities of different regions in India. Tailored

interventions are needed to protect agriculture, public health, and urban infrastructure from the growing risks associated with rising Summer Days.

This study underscores the need for proactive, region-specific measures to enhance climate resilience in India, while also challenging common misconceptions about resilience—especially those embedded in formal and nonformal education systems [25,26]. By linking scientific projections with actionable adaptation strategies, it contributes to more effective responses to global warming and potential economic restructuring [27].

5. Conclusions

This study presents a comprehensive spatio-temporal assessment of Summer Days across India under varying Indian Warming Targets (IWTs), using multi-model ensembles from CORDEX-SA under RCP4.5 and RCP8.5 scenarios. The findings indicate that increasing global temperatures will significantly alter the frequency and spatial distribution of Summer Days, with notable regional variations. North-Central and North-East India are projected to experience the largest increases in summer days, while the East and West coastal regions are likely to sustain persistently high temperatures throughout the year.

The analysis, based on robust non-parametric statistical methods such as the Mann–Kendall test, Modified Mann–Kendall test, Sen’s Slope Estimator, and Pettitt–Mann–Whitney test, reveals a statistically significant rise in summer days across all scenarios, with accelerated trends under higher warming targets in the RCP8.5 scenario. The results underscore the heightened risks posed by regional warming, even as global climate policies target a 2 °C threshold. This study also employs the Reliability Ensemble Averaging (REA) technique to quantify uncertainty, highlighting the necessity of combining multiple model simulations for precise regional climate impact assessments.

The projected increase in the frequency of summer days necessitates targeted region-specific adaptation strategies to mitigate adverse impacts. For North-Central and North-East India, where the increase in summer days is most pronounced, public health interventions such as Heat Action Plans (HAPs), community cooling centers, and early warning systems are essential to minimize heat-related health risks, particularly for vulnerable populations.

In the agricultural sector, the adoption of heat-resilient crop varieties and improved water management practices is critical to maintaining productivity in regions facing intensified heat stress. Practices such as drip irrigation and rainwater harvesting should be prioritized to address increased evapotranspiration and ensure water availability during prolonged heat periods. Urban areas, particularly along the East and West coasts, must implement measures to combat the urban heat island effect [28], including urban afforestation, the use of cool roofing materials, and reflective pavements to reduce localized temperature extremes [29]. Enhancing green infrastructure and increasing urban canopy coverage can further improve thermal comfort in cities [30]. Additionally, the rising demand for cooling will stress energy systems, necessitating investments in energy-efficient cooling technologies, renewable energy solutions [31], and robust grid infrastructure to ensure reliability during peak demand periods [32].

These region-specific recommendations provide actionable guidance for policymakers and stakeholders to address the multifaceted risks associated with rising temperatures [33]. Proactive adaptation measures tailored to the unique vulnerabilities of different regions are essential to safeguard public health, sustain agricultural productivity, and enhance urban livability and energy resilience [33]. The insights from this study underscore the importance of building regional and local climate resilience to mitigate the escalating challenges posed by global climate change, thereby supporting sustainable development goals.

Author Contributions: Conceptualization, D.K.P., M.C. and R.A. Methodology, D.K.P. and R.A. Software, S.S. and S.A. Validation, R.A. and S.A. Formal analysis, A.K. Investigation, D.K.P. and S.S. Resources, R.A. and S.A. Data curation, S.S. and S.A. Writing—original draft preparation, D.K.P. and R.A. Writing—review and editing, A.K. and S.A. Visualization, S.S. and S.A. Supervision, R.A. Project administration, R.A. Funding acquisition, R.A. and S.A. All authors have read and agreed to the published version of the manuscript.

Funding: This research was partially supported by the Deanship of Scientific Research at King Khalid funding this work through a large research group (project group number RGP 1/219/45) and JST SICORP, grant number JPMJSC23A1.

Data Availability Statement: Data can be provided upon request.

Acknowledgments: This work was supported by JST Grant Number JPMJPF2108 and Sakura Science Indian Young Researchers Invitation Program (JPMJI2427). We are thankful to Hokkaido University, Poornima University and King Khalid University for research support.

Conflicts of Interest: The authors declare no conflict of interest.

References

- Hawkins, E.; Frame, D.; Harrington, L.; Joshi, M.; King, A.; Rojas, M.; Sutton, R. Observed Emergence of the Climate Change Signal: From the Familiar to the Unknown. *Geophys. Res. Lett.* **2020**, *47*, e2019GL086259. [\[CrossRef\]](#)
- Tabari, H. Climate change impact on flood and extreme precipitation increases with water availability. *Sci. Rep.* **2020**, *10*, 13768. [\[CrossRef\]](#) [\[PubMed\]](#)
- Liu, K.; Harrison, M.T.; Yan, H.; Liu, D.L.; Meinke, H.; Hoogenboom, G.; Wang, B.; Peng, B.; Guan, K.; Jaegermeyr, J.; et al. Silver lining to a climate crisis in multiple prospects for alleviating crop waterlogging under future cli-mates. *Nat. Commun.* **2023**, *14*, 765. [\[CrossRef\]](#) [\[PubMed\]](#)
- Weiskopf, S.R.; Rubenstein, M.A.; Crozier, L.G.; Gaichas, S.; Griffis, R.; Halofsky, J.E.; Hyde, K.J.W.; Morelli, T.L.; Morissette, J.T.; Muñoz, R.C.; et al. Climate change effects on biodiversity, ecosystems, ecosystem services, and natural resource management in the United States. *Sci. Total Environ.* **2020**, *733*, 137782. [\[CrossRef\]](#)
- Malhi, G.S.; Kaur, M.; Kaushik, P. Impact of Climate Change on Agriculture and Its Mitigation Strategies: A Review. *Sustainability* **2021**, *13*, 1318. [\[CrossRef\]](#)
- Hussain, S.; Hussain, E.; Saxena, P.; Sharma, A.; Thathola, P.; Sonwani, S. Navigating the impact of climate change in India: A perspective on climate action (SDG13) and sus-tainable cities and communities (SDG11). *Front. Sustain. Cities* **2023**, *5*, 1308684. [\[CrossRef\]](#)
- Dimitrova, A.; Ingole, V.; Basagaña, X.; Ranzani, O.; Milà, C.; Ballester, J.; Tonne, C. Association between ambient temperature and heat waves with mortality in South Asia: Systematic review and meta-analysis. *Environ. Int.* **2021**, *146*, 106170. [\[CrossRef\]](#)
- Mikó, E.; Donyina, G.A.; Baccouri, W.; Tóth, V.; Flórián, K.; Gyalai, I.M.; Yüksel, G.; Köteles, D.; Srivastava, V.; Wanjala, G. One health agriculture: Heat stress mitigation dilemma in agriculture. *One Health* **2025**, *20*, 100966. [\[CrossRef\]](#)
- Mishra, V.; Dangar, S.; Tiwari, V.M.; Lall, U.; Wada, Y. Summer monsoon drying accelerates India's groundwater depletion under climate change. *Earth's Future* **2024**, *12*, e2024EF004516. [\[CrossRef\]](#)
- Mohanasundaram, M.; Abhiyant, T.; Vijay, L.; Andreas, M.; Arvind, K.S.; Upasona, G.; Debkumar, P.; Chandrakant, L. Heat Stress in India: A Review. *Prev. Med. Res. Rev.* **2024**, *1*, 140–147.
- Varikoden, H.; Mujumdar, M.; Revadekar, J.V.; Sooraj, K.P.; Ramarao, M.V.S.; Sanjay, J.; Krishnan, R. Assessment of regional downscaling simulations for long term mean, excess and deficit Indian Summer Monsoons. *Glob. Planet. Change* **2018**, *162*, 28–38. [\[CrossRef\]](#)
- Demissie, T.A.; Sime, C.H. Assessment of the performance of CORDEX regional climate models in simulating rainfall and air temperature over southwest Ethiopia. *Heliyon* **2021**, *7*, e07791. [\[CrossRef\]](#) [\[PubMed\]](#)
- Singh, A.; Patwardhan, A. Spatio-Temporal Distribution of Extreme Weather Events in India. *APCBEE Procedia* **2012**, *1*, 258–262. [\[CrossRef\]](#)
- Paul, A.R.; Maity, R. Future projection of climate extremes across contiguous northeast India and Bangladesh. *Sci. Rep.* **2023**, *13*, 15616. [\[CrossRef\]](#) [\[PubMed\]](#)
- Grigorieva, E.; Livenets, A.; Stelmakh, E. Adaptation of Agriculture to Climate Change: A Scoping Review. *Climate* **2023**, *11*, 202. [\[CrossRef\]](#)
- Datta, P.; Behera, B.; Rahut, D.B. Climate change and Indian agriculture: A systematic review of farmers' perception, adaptation, and transformation. *Environ. Chall.* **2022**, *8*, 100543. [\[CrossRef\]](#)

17. Yaduvanshi, A.; Zaroug, M.; Bendapudi, R.; New, M. Impacts of 1.5 °C and 2 °C global warming on regional rainfall and temperature change across India. *Environ. Res. Commun.* **2019**, *1*, 125002. [[CrossRef](#)]
18. Maharana, P. Projected change in the rainfall behaviour over Odisha. *J. Water Clim. Change* **2024**, *15*, 4517–4535. [[CrossRef](#)]
19. Li, K.; Pan, J.; Xiong, W.; Xie, W.; Ali, T. The impact of 1.5 °C and 2.0 °C global warming on global maize production and trade. *Sci. Rep.* **2022**, *12*, 17268. [[CrossRef](#)]
20. Bai, T.; Fan, L.; Song, G.; Song, H.; Ru, X.; Wang, Y.; Zhang, H.; Min, R.; Wang, W. Effects of Land Use/Cover and Meteorological Changes on Regional Climate under Different SSP-RCP Scenarios: A Case Study in Zhengzhou, China. *Remote Sens.* **2023**, *15*, 2601. [[CrossRef](#)]
21. Huang, S.; Leng, G.; Huang, Q.; Xie, Y.; Liu, S.; Meng, E.; Li, P. The asymmetric impact of global warming on US drought types and distributions in a large ensemble of 97 hydro-climatic simulations. *Sci. Rep.* **2017**, *7*, 5891. [[CrossRef](#)]
22. Chauhan, A.S.; Singh, S.; Maurya, R.K.S.; Rani, A.; Danodia, A. Spatio-temporal and trend analysis of rain days having different intensity from 1901–2020 at regional scale in Haryana, India. *Results Geophys. Sci.* **2022**, *10*, 100041. [[CrossRef](#)]
23. Arulalan, T.; AchutaRao, K.; Sagar, A.D. Climate science to inform adaptation policy: Heat waves over India in the 1.5°C and 2°C warmer worlds. *Clim. Change* **2023**, *176*, 64. [[CrossRef](#)]
24. Islam, S.; Karipot, A.; Bhawar, R.; Sinha, P.; Kedia, S.; Khare, M. Urban heat island effect in India: A review of current status, impact and mitigation strategies. *Discov. Cities* **2024**, *1*, 34. [[CrossRef](#)]
25. Calvente, A.; Kharrazi, A.; Kudo, S.; Savaget, P. Non-Formal Environmental Education in a Vulnerable Region: Insights from a 20-Year Long Engagement in Petrópolis, Rio de Janeiro, Brazil. *Sustainability* **2018**, *10*, 4247. [[CrossRef](#)]
26. Kharrazi, A.; Kudo, S.; Allasiw, D. Addressing Misconceptions to the Concept of Resilience in Environmental Education. *Sustainability* **2018**, *10*, 4682. [[CrossRef](#)]
27. Zhang, S.; Yu, Y.; Kharrazi, A.; Ren, H.; Ma, T. Quantifying the synergy and trade-offs among economy–energy–environment–social targets: A perspective of industrial restructuring. *J. Environ. Manag.* **2022**, *316*, 115285. [[CrossRef](#)] [[PubMed](#)]
28. Ulpiani, G.; Treville, A.; Bertoldi, P.; Vettors, N.; Barbosa, P.; Feyen, L.; Naumann, G.; Santamouris, M. Are cities taking action against urban overheating? Insights from over 7500 local climate actions. *One Earth* **2024**, *7*, 848–866. [[CrossRef](#)]
29. de Quadros, B.M.; Mizgier, M.G.O. Urban green infrastructures to improve pedestrian thermal comfort: A systematic review. *Urban For. Urban Green.* **2023**, *88*, 128091. [[CrossRef](#)]
30. Khosravi, F.; Lowes, R.; Ugalde-Loo, C.E. Cooling is hotting up in the UK. *Energy Policy* **2023**, *174*, 113456. [[CrossRef](#)]
31. Nebey, A.H. Recent advancement in demand side energy management system for optimal energy utilization. *Energy Rep.* **2024**, *11*, 5422–5435. [[CrossRef](#)]
32. Singh, S.; Avtar, R.; Jain, A.; Alsulamy, S.; Ouda, M.M.; Kharrazi, A. Identifying Micro-Level Pollution Hotspots Using Sentinel-5P for the Spatial Analysis of Air Quality Degradation in the National Capital Region, India. *Sustainability* **2025**, *17*, 2241. [[CrossRef](#)]
33. Supe, H.; Abhishek, A.; Avtar, R. Assessment of the solar energy–agriculture–water nexus in the expanding solar energy industry of India: An initiative for sustainable resource management. *Heliyon* **2024**, *10*, e23125. [[CrossRef](#)] [[PubMed](#)]

Disclaimer/Publisher’s Note: The statements, opinions and data contained in all publications are solely those of the individual author(s) and contributor(s) and not of MDPI and/or the editor(s). MDPI and/or the editor(s) disclaim responsibility for any injury to people or property resulting from any ideas, methods, instructions or products referred to in the content.